

# Consistency between renormalization group running of chiral operator and counting rule

## — Case of chiral pion production operator —

Satoshi X. Nakamura<sup>1,2,\*</sup>

<sup>1</sup>*Theory Group, TRIUMF, 4004 Wesbrook Mall, Vancouver, BC V6T 2A3, Canada*

<sup>2</sup>*Instituto de Física, Universidade de São Paulo, São Paulo -SP, 05508-090, Brazil*

(Dated: August 14, 2021)

### Abstract

In nuclear chiral perturbation theory ( $\chi$ PT), an operator is defined in a space with a cutoff which may be varied within a certain range. The operator runs as a result of the variation of the cutoff [renormalization group (RG) running]. In order for  $\chi$ PT to be useful, the operator should run in a way consistent with the counting rule; that is, the running of chiral counter terms have to be of natural size. We vary the cutoff using the Wilsonian renormalization group (WRG) equation, and examine this consistency. As an example, we study the  $s$ -wave pion production operator for  $NN \rightarrow d\pi$ , derived in  $\chi$ PT. We demonstrate that the WRG running does not generate any chiral-symmetry-violating (CSV) interaction, provided that we start with an operator which does not contain a CSV term. We analytically show how the counter terms are generated in the WRG running in case of the infinitesimal cutoff reduction. Based on the analytic result, we argue a range of the cutoff variation for which the running of the counter terms is of natural size. Then, we numerically confirm this.

PACS numbers: 05.10.Cc, 25.10.+s, 11.30.Rd, 13.60.Le, 25.40.-h

Keywords: renormalization group, chiral perturbation theory, pion production

---

\*Electronic address: [satoshi@jlab.org](mailto:satoshi@jlab.org); Current affiliation: Excited Baryon Analysis Center (EBAC), Thomas Jefferson National Accelerator Facility, Newport News, VA 23606, USA

## I. INTRODUCTION

In nuclear chiral perturbation theory ( $\chi$ PT), operators (*e.g.*, nuclear force, electroweak current and pion production operator) are derived from a chiral Lagrangian following a counting rule. Many processes in few-nucleon system have been successfully described by these chiral operators, establishing the validity of this approach. [1, 2] The chiral nuclear operators are defined in a model space with a certain cutoff. The cutoff has a physical meaning and its choice is not arbitrary. Given a long-range (*e.g.*, pion exchange) mechanism, the cutoff should be smaller than the scale where the details of shorter-range mechanisms are resolved. For example, in describing a nuclear operator with pion-exchange mechanisms plus contact terms, the cutoff should be smaller than the  $\rho$  meson mass. Also, the cutoff should not be so small that the long-range mechanism is not fully taken into account. Although not arbitrary, the cutoff still may be varied within a physically reasonable region. As a result of the variation of the cutoff, an operator (more specifically, couplings of counter terms) runs so that observables are cutoff-independent [renormalization group (RG) running]. A question here is whether the running of the counter terms is consistent with the counting rule. Stated differently, we wonder whether the counter terms run with keeping the size of the couplings natural [ $\mathcal{O}(1)$ ]. This consistency is a necessary condition for the counting rule to be useful because, if not satisfied, the counting rule does not correctly reflect the ordering of the importance of the counter terms.

In order to address the question concerning the consistency between the RG running and the counting rule, we propose to use a RG equation which controls the running of an operator so that Green's functions are unchanged. Wilsonian RG (WRG) equation is such an equation. For studying the RG running, we consider it the most appropriate to use the WRG equation because we have the following beneficial points: (i) The WRG equation is consistent with the derivation of the effective Lagrangian with a path integral, see Sec. II; (ii) It is guaranteed that no chiral-symmetry-violating (CSV) interactions are generated by the WRG running, <sup>1</sup> provided that no CSV term exists (*e.g.*, the operator vanishes at threshold in the chiral limit) in both a transition operator and a nuclear force before the RG running, see Sec. IV; (iii) Since we have the RG running of the operator which correctly reflects the high-momentum states integrated out, we can study the convergence of the chiral expansion of the RG running. Our usage of the WRG equation is different from Refs. [3, 4] in which the scaling behavior of each interaction near the fixed point is identified with power counting. What we would like to do is also different from Refs. [5, 6]

---

<sup>1</sup> In Sec. II, we will explain in more detail what we mean by “no CSV terms are generated in the WRG running”.

where the renormalizability of the leading order (LO) chiral  $NN$  potential over a very wide range of the cutoff is examined. We apply the WRG equation to a set of operators derived with an established power counting, and then examine the internal consistency between the RG running and the counting rule over a physically reasonable range of the cutoff. In the above RG analyses[3, 4, 5, 6], the authors are *not* primarily interested in the actual size of the running for a physically reasonable range of the cutoff. We are interested in the actual size of the RG running and its consistency with the counting rule. One may naively expect that this kind of calculation only generates the counter terms which scale as  $\propto 1/\Lambda$  ( $\Lambda$  : cutoff). We will semi-analytically show that this expectation is not always the case, and find a size of the variation of  $\Lambda$  for which this expectation holds true. Also, we argue that the RG running is consistent with the counting rule if we vary the cutoff smaller than this size; otherwise, the RG running could be divergent. This argument is also consistent with the divergent RG running of some contact  $NN$  interactions which was found in Ref. [5] (*e.g.*, see Fig. 2 of the paper). The physically reasonable range of the cutoff is consistent with the size of the variation of  $\Lambda$  which we semi-analytically find.

We quantitatively confirm the above qualitative analysis by a numerical calculation.<sup>2</sup> In the numerical calculation, we use a phenomenological nuclear force rather than a  $\chi$ PT-based nuclear force. A reason is that chiral  $NN$ -potentials available[9] have relatively small cutoffs ( $\Lambda \sim 500$  MeV) and are not very appropriate to study the WRG running in the cutoff range considered in this work ( $500 \text{ MeV} \leq \Lambda \leq 800 \text{ MeV}$ ). Phenomenological  $NN$ -potentials such as the CD-Bonn  $NN$ -potential [10] which we use are not based on the chiral Lagrangian. However, these potentials have been often used with chiral operators (electroweak currents, pion production operators) to calculate matrix elements (hybrid approach). This hybrid approach has been used extensively, through which its usefulness has been established[2]. Despite the phenomenological success of the hybrid approach, there is still a concern about the consistency between the nuclear force and the chiral transition operators. In this context, the present RG analysis may provide an interesting test for the hybrid approach. This is because if a CSV term is generated in the WRG running, then the result signals that the nuclear force contains a numerically significant CSV component and one has to doubt the validity of the hybrid approach.

This paper is organized as follows. In Sec. II, we first develop a formal apparatus to address the question of how to evolve the operator for changing  $\Lambda$ , using the WRG equation. In Sec. III, we present expressions for the chiral next-to-leading order (NLO)  $s$ -wave  $\pi$ -

---

<sup>2</sup> Similar analyses addressing the RG running and the naturalness of the counter terms in the  $NN$  interaction are found in Refs. [7, 8]; the WRG equation is used in Ref. [7] while a unitary transformation is used in Ref. [8].

production operator [11] to which we apply the WRG analysis as a demonstration, and address the question of the consistency. The operator we use is based on the heavy-baryon  $\chi$ PT with a revised power counting scheme [12] which treats the large incoming nucleon momentum as a separate large energy/momentum scale (see, *e.g.*, Ref. [13] for a treatment using the original Weinberg counting [14]). We use the revised power counting throughout this work unless otherwise specifically stated. In Sec. IV, we reduce the (sharp) cutoff of the chiral  $\pi$ -production operator by the infinitesimal amount using the WRG equation and the chiral LO nuclear force. We obtain analytic expressions which show that the WRG equation indeed induces the running of the chiral counter terms; no CSV terms are generated. In Sec. V, in order to quantitatively address the RG running, we reduce the cutoff of the  $\pi$ -production operator from  $\Lambda = 800$  MeV down to  $\Lambda = 700, 600$  and  $500$  MeV using the WRG equation with a phenomenological nuclear force. As a result we obtain numerically the corresponding effective operators. Then, we try to reproduce the effective RG low-momentum operator<sup>3</sup> by calculating another operator consisting of the chiral NLO operator and the chiral counter terms; the chiral counter terms are introduced following the counting rule. The counter terms are accompanied by unknown coefficients, the so-called low-energy constants (LECs), which are determined by fitting to the low-momentum operator. We will show that the running of the operator with  $\Lambda$  is, to a very high precision, captured by the lowest order counter term. Finally, we summarize our findings in Sec. VI. Some calculations are relegated to an Appendix.

## II. WILSONIAN RENORMALIZATION GROUP EQUATION FOR TRANSITION OPERATOR

The WRG equation is an equation which is designed to control the running of a set of operators, as a result of the cutoff reduction, so that Green's functions are unchanged. At first, we state why we use the WRG equation to reduce the cutoff. An effective Lagrangian can be obtained formally via a path integral formulation based on the Lagrangian of the underlying, more fundamental theory. One integrates out the high energy degrees of freedom using the path integral. When integrating out the high momentum states of the nucleon in the heavy-baryon  $\chi$ PT Lagrangian, we can also use the path integral. This procedure is equivalent to solving the WRG equation derived below; we will state more on this later. Thus one way of reducing the cutoff consistently with effective field theory is through using the WRG equation. It is not a priori guaranteed that the WRG running of the counter terms

---

<sup>3</sup> In this work, we will use the term “low-momentum interaction” to refer to an effective interaction obtained with the Wilsonian renormalization group equation.

is consistent with the counting rule, and thus we consider it worthwhile examining. We will see that the WRG running is consistent when the cutoff is changed within a physically reasonable range; otherwise, not necessarily consistent.

Contrary to the approach in the above paragraphs, some previous works did not use a RG equation for studying RG running. Instead, for a given cutoff, the (leading) counter term was fixed so that some observables were reproduced. Repeating this procedure over a certain range of the cutoff leads to the RG running of the counter term. In this procedure, it is assumed that the running of the (leading) counter term simulates the high momentum states integrated out. However, one could fix the coupling of a higher-order counter term, instead of the leading term, so that some observables were reproduced. Without using a RG equation, it is impossible to know which counter term is running. Furthermore, our approach based on the WRG equation is more advantageous than the above RG analyses on the following two points: (i) it is guaranteed that no CSV operator is generated in the RG running, provided that no CSV term exists before the RG running; (ii) the RG running of the operator which exactly reflects the high momentum states integrated out is at hand, and thus we can examine whether the RG running is captured by a series of the chiral counter terms consistently with the counting rule. We detail the above statement (i) in the following. The chiral operators in the nuclear  $\chi$ PT are not chiral invariant in the sense that the original Lagrangian is invariant under chiral transformations. We take advantage of the chiral symmetry by deriving the operators from the chiral Lagrangian; the parameterization of the operators is given by the chiral Lagrangian. After the WRG running, if the operators are still accurately parameterized by the same parameterization, we state that no CSV interactions are generated. We do not address the chiral symmetry invariance of the original chiral Lagrangian in the RG running. Here we are interested in nuclear operators based on  $\chi$ PT, which is actually used in practical calculations, and their WRG running. As far as we examine the WRG running of the  $\chi$ PT-based operators with the cutoff, no CSV term is generated.

As stated in the previous paragraph, the WRG equation can be derived using the path integral. The present author derived the WRG equation for the  $NN$  interaction in this way in Ref. [7]. The WRG equation for a transition operator ( $\pi$  production operator in our case) can also be derived in essentially the same way, whereas we can also derive it in a simpler way as detailed in Ref. [15] (Appendix A of that reference).<sup>4</sup> Here we derive the WRG equation following Ref. [15] for simplicity *without* using the partial wave decomposition that

---

<sup>4</sup> In Ref. [15], the WRG equation was derived as a sufficient condition of the cutoff independence of a matrix element. Recently, it was shown that the same WRG equation is also necessary-sufficient condition, if one imposes the cutoff independence of the five point Green function [16].

was used in Ref. [15]. We start with a matrix element in which the transition operator is defined in a model space spanned by plane wave states of the two-nucleon system. The maximum magnitude of the relative momentum in the model space is given by the cutoff,  $\Lambda$ . The matrix element of an operator  $O$  is given by

$$\langle \mathbf{p}' | O | \mathbf{p} \rangle = \int_0^\Lambda d\mathbf{k} \int_0^\Lambda d\mathbf{k}' \psi_{\mathbf{p}'}^\dagger(\mathbf{k}') O(\mathbf{k}', \mathbf{k}) \psi_{\mathbf{p}}(\mathbf{k}) , \quad (1)$$

where  $\psi_{\mathbf{p}}(\mathbf{k})$  [ $\psi_{\mathbf{p}'}(\mathbf{k}')$ ] is the wave function for the initial (final) two-nucleon state. The wave functions are derived from a low-momentum  $NN$  interaction with the same cutoff  $\Lambda$ . The quantity  $\mathbf{p}$  ( $\mathbf{p}'$ ) is the on-shell relative momentum for the initial (final) two-nucleon state. The on-shell momentum is related to the energy ( $E$ ) for the relative motion of the two nucleons through  $p = |\mathbf{p}| = \sqrt{ME}$ , where  $M$  is the nucleon mass. We denote the transition operator  $O(\mathbf{k}', \mathbf{k})$ , where  $\mathbf{k}$  ( $\mathbf{k}'$ ) is the relative off-shell momentum of the two-nucleon system before (after) the interaction  $O$ .

We differentiate both sides of Eq. (1) with respect to  $\Lambda$  and impose the renormalization condition that the matrix element is invariant under cutoff changes, *i.e.*,  $d\langle O \rangle / d\Lambda = 0$ . This gives the WRG equation for the low-momentum transition operator (with arguments now explicitly shown),

$$\begin{aligned} & \frac{\partial O_\Lambda(\mathbf{k}', \mathbf{k}; p', p)}{\partial \Lambda} \\ &= M \int \frac{d\Omega_{\hat{\Lambda}}}{(2\pi)^3} \left( \frac{O_\Lambda(\mathbf{k}', \Lambda; p', p) V_\Lambda(\Lambda, \mathbf{k}; p)}{1 - p^2/\Lambda^2} + \frac{V_\Lambda(\mathbf{k}', \Lambda; p') O_\Lambda(\Lambda, \mathbf{k}; p', p)}{1 - p'^2/\Lambda^2} \right) , \quad (2) \end{aligned}$$

with  $\hat{\Lambda} \equiv \Lambda/\Lambda$ . The low-momentum  $NN$ -potential,  $V_\Lambda(\mathbf{k}', \mathbf{k}; p)$ , evolves according to the WRG equation for the  $NN$  potential [3, 7]. The low-momentum operator acquires a dependence on both the initial and final on-shell momenta,  $p$  and  $p'$ , as indicated by Eq. (2).

The WRG equation is solved in order to derive  $O_\Lambda$  from  $O = O_{\bar{\Lambda}}$  with a cutoff  $\bar{\Lambda} (> \Lambda)$ . The solution (in integral form) of the WRG equation is (for later convenience now given with partial wave decomposition),

$$\begin{aligned} O_\Lambda^{(\beta, \alpha)} &= \eta \left( O_{\bar{\Lambda}}^{(\beta, \alpha)} + O_{\bar{\Lambda}}^{(\beta, \alpha)} \frac{1}{E - \lambda H_{\bar{\Lambda}}^{(\alpha)}} \lambda V_{\bar{\Lambda}}^{(\alpha)} + V_{\bar{\Lambda}}^{(\beta)} \lambda \frac{1}{E' - H_{\bar{\Lambda}}^{(\beta)} \lambda} O_{\bar{\Lambda}}^{(\beta, \alpha)} \right. \\ &\quad \left. + V_{\bar{\Lambda}}^{(\beta)} \lambda \frac{1}{E' - H_{\bar{\Lambda}}^{(\beta)} \lambda} O_{\bar{\Lambda}}^{(\beta, \alpha)} \frac{1}{E - \lambda H_{\bar{\Lambda}}^{(\alpha)}} \lambda V_{\bar{\Lambda}}^{(\alpha)} \right) \eta , \quad (3) \end{aligned}$$

where  $H_{\bar{\Lambda}}^{(\alpha)}$  and  $V_{\bar{\Lambda}}^{(\alpha)}$  are the full Hamiltonian and the  $NN$ -interaction for partial wave  $\alpha$ , defined in the model space with cutoff  $\bar{\Lambda}$ . The operator  $O_{\bar{\Lambda}}^{(\beta, \alpha)}$  generates a transition from a partial wave  $\alpha$  to  $\beta$ . The projection operators  $\eta$  and  $\lambda$  are defined by

$$\eta = \int \frac{\bar{k}^2 d\bar{k}}{2\pi^2} |\bar{k}\rangle \langle \bar{k}| , \quad \bar{k} \leq \Lambda , \quad (4)$$

$$\lambda = \int \frac{\bar{k}^2 d\bar{k}}{2\pi^2} |\bar{k}\rangle \langle \bar{k}|, \quad \Lambda < \bar{k} \leq \bar{\Lambda}, \quad (5)$$

where  $|\bar{k}\rangle$  represents the radial part of the free two-nucleon states with the relative momentum  $\bar{k}$ . Equation (3) is the same as for the effective operator in the Bloch-Horowitz formalism [17]. Similarities between the projection formalisms (*e.g.*, Bloch-Horowitz and Lee-Suzuki formalisms) and RG techniques have been explored previously in other contexts, see, *e.g.*, Refs. [18, 19].

### III. CHIRAL $s$ -WAVE PION PRODUCTION OPERATOR

Here we present the  $\chi$ PT-based  $s$ -wave pion production operator for the  $NN \rightarrow d\pi$  reaction near threshold. We will start our RG analysis with this operator, and examine the consistency between the RG running of this chiral operator and the counting rule. We use the operator from Ref. [11], which was derived using the modified power counting rule proposed in Ref. [12]. In this counting the large relative momentum ( $p = \sqrt{Mm_\pi}$ ) of the incoming nucleons is counted as an additional large energy-momentum scale of the problem, leading to an expansion in  $\chi \sim \sqrt{\frac{m_\pi}{M}}$  rather than in the  $\frac{m_\pi}{M}$  of the original Weinberg counting [14]. The leading-order (LO) operators are given by the (nucleon recoil) one-body operator and rescattering via the Weinberg-Tomozawa (WT) interaction. At the next-to-leading order (NLO), several loop diagrams start to contribute, the sum of which does not vanish in the chiral limit when sandwiched between wave functions [20], leading to a divergent matrix element. A solution to this dilemma was proposed in Ref. [11], where it was shown that the WT term and its recoil correction, taken together with a pion exchange extracted from the initial or final state wave functions, contribute an irreducible NLO diagram that exactly cancels the offending divergence of the pion loop diagrams.<sup>5</sup> We are left with WT rescattering, with its energy dependence replaced by the on-shell value, and no CSV term. The result is that, up to NLO, we consider the (nucleon recoil) one-body plus a modified WT rescattering term (WT'), the latter a factor 4/3 stronger than the original WT term [11]. These operators are given (in momentum space) by

$$O_{\text{WT}'} = \frac{g_A \omega_q}{4f_\pi^3} \varepsilon^{abc} \tau_1^b \tau_2^c \left( \frac{\boldsymbol{\sigma}_1 \cdot (\mathbf{k}'_1 - \mathbf{k}_1)}{m_\pi'^2 + (\mathbf{k}'_1 - \mathbf{k}_1)^2} - \frac{\boldsymbol{\sigma}_2 \cdot (\mathbf{k}'_2 - \mathbf{k}_2)}{m_\pi'^2 + (\mathbf{k}'_2 - \mathbf{k}_2)^2} \right), \quad (6)$$

$$O_{\text{1B}} = \frac{-i g_A \omega_q (2\pi)^3}{4M f_\pi} \left[ \tau_1^a \delta^{(3)}(\mathbf{k}'_2 - \mathbf{k}_2) \boldsymbol{\sigma}_1 \cdot (\mathbf{k}_1 + \mathbf{k}'_1) + \tau_2^a \delta^{(3)}(\mathbf{k}'_1 - \mathbf{k}_1) \boldsymbol{\sigma}_2 \cdot (\mathbf{k}_2 + \mathbf{k}'_2) \right], \quad (7)$$

---

<sup>5</sup> In an irreducible diagram, the nucleons of any two-nucleon cut are off shell by  $\sim m_\pi$ , *i.e.*, an irreducible diagram cannot be split into smaller diagrams with all external nucleons on-shell.

where  $m'_\pi{}^2 = \frac{3}{4}m_\pi^2$  and  $\omega_q$  is the energy of the emitted pion. The momentum for  $i$ -th nucleon in the initial (final) state is denoted by  $\mathbf{k}_i$  ( $\mathbf{k}'_i$ ). The axial-vector coupling constant and the pion decay constant are denoted by  $g_A$  and  $f_\pi$ , respectively. We have employed the so-called fixed-kinematics approximation, in which the energy transfer is equally shared between the incoming nucleons and fixed to the threshold value  $m_\pi/2$ , where  $m_\pi$  is the pion mass. Other choices are possible [21], but we will take this simple prescription here, and relegate an investigation regarding this issue to future work.

When we let the one-body operator run according to the WRG equation, we obtain a low-momentum operator with a kink structure. (See Fig. 1.) The origin of the kink is high momentum components of the bare one-body operator that are integrated out. We explain here this point more using the WRG equation [Eq. (2)]. When the cutoff is reduced by  $\delta\Lambda$ , the running of the operator due to the momentum shell of the one-body operator integrated out is given up to the order of  $\delta\Lambda$  as

$$\delta O_\Lambda(\mathbf{k}', \mathbf{k}; p', p) = M \int \frac{d\Omega_{\hat{\Lambda}}}{(2\pi)^3} \left( \frac{O_{1B\Lambda}(\mathbf{k}', \Lambda) V_\Lambda(\Lambda, \mathbf{k}; p)}{1 - p^2/\Lambda^2} + \frac{V_\Lambda(\mathbf{k}', \Lambda; p') O_{1B\Lambda}(\Lambda, \mathbf{k})}{1 - p'^2/\Lambda^2} \right) \delta\Lambda, \quad (8)$$

where the relative nucleon momenta before and after the insertion of  $O_{1B}$  are  $\mathbf{k} = (\mathbf{k}_1 - \mathbf{k}_2)/2$  and  $\mathbf{k}' = (\mathbf{k}'_1 - \mathbf{k}'_2)/2$ , respectively, and they are related to the pion momentum ( $\mathbf{q}$ ) through  $\mathbf{k}' = \mathbf{k} - \frac{\mathbf{q}}{2}$ . The first term in r.h.s. of Eq. (8) is non-vanishing only when  $\mathbf{k}' + \frac{\mathbf{q}}{2} = \Lambda$  because of the  $\delta$ -function in Eq. (7). This means that the shift of the operator  $[\delta O_\Lambda(\mathbf{k}', \mathbf{k}; p', p)]$  is generated only for  $|\mathbf{k}'| \geq \Lambda - \frac{q}{2}$ . Similarly, the second term in r.h.s. of Eq. (8) induces the running of the operator only for  $|\mathbf{k}| \geq \Lambda - \frac{q}{2}$ ; the kink structure is created in this way. On the other hand, if  $O_{1B}$  in Eq. (8) is replaced by  $O_{WT'}$  [Eq. (6)], then the shift of the operator  $[\delta O_\Lambda(\mathbf{k}', \mathbf{k}; p', p)]$  is induced for all values of  $\mathbf{k}$  and  $\mathbf{k}'$  because  $O_{WT'}$  does not contain the  $\delta$ -function. Thus the kink structure does not mean the strong dependence of the operator on the cutoff. Rather, it originates from the  $\delta$ -function in the one-body operator, or in other words, from the way we have chosen to define the transition operators and wave functions. We could have chosen a set of transition operators without the one-body operator by extracting the one-pion-exchange (or some other) mechanism, which is nearest the one-body operator, from the wave function and connecting it to the one-body operator; a two-body operator is formed in this way. The RG running of this operator does not generate the kink structure. However, we use the one-body operator here because it is often used in practical calculations and the kink part will contribute only marginally to the RG running for the reaction near threshold ( $|\mathbf{q}| \sim 0$ ) which is of our interest here. (At  $|\mathbf{q}| = 0$ , the kink does not appear.) When fitting the counter terms to the RG low-momentum operator, we simply omit the kink structure which obviously cannot be simulated by counter terms. As we said, the kink part contributes only marginally to the RG running, and thus we do not consider this omission to be influential on a conclusion of this work.



#### IV. RENORMALIZATION GROUP RUNNING, CHIRAL SYMMETRY AND COUNTER TERMS

We study the RG running, guided by the WRG equation, of the  $\pi$  production operator presented in the previous section. In  $\chi$ PT, the running coupling constants of the chiral counter terms should capture the WRG running of the operator. The leading order counter terms (with one spatial derivative) from the heavy-baryon  $\chi$ PT Lagrangian, relevant to this work, are given as [22]

$$\begin{aligned} \mathcal{L}_{ct} = & \frac{i}{2Mf_\pi} \frac{g_A}{Mf_\pi^2} \left\{ \hat{D}_{1a} N^\dagger (\boldsymbol{\tau} \cdot \hat{\boldsymbol{\pi}} \vec{\sigma} \cdot \vec{\nabla} - \vec{\sigma} \cdot \overleftarrow{\nabla} \boldsymbol{\tau} \cdot \hat{\boldsymbol{\pi}}) N N^\dagger N \right. \\ & + \hat{D}_{1b} N^\dagger \boldsymbol{\tau} \cdot \hat{\boldsymbol{\pi}} \vec{\sigma} N \cdot N^\dagger (\vec{\nabla} - \overleftarrow{\nabla}) N + \hat{D}_{1c} N^\dagger (\boldsymbol{\tau} \cdot \hat{\boldsymbol{\pi}} \vec{\nabla} - \overleftarrow{\nabla} \boldsymbol{\tau} \cdot \hat{\boldsymbol{\pi}}) N \cdot N^\dagger \vec{\sigma} N \\ & + \hat{D}_{1d} N^\dagger \boldsymbol{\tau} \cdot \hat{\boldsymbol{\pi}} N N^\dagger \vec{\sigma} \cdot (\vec{\nabla} - \overleftarrow{\nabla}) N + i \hat{D}_{1e} \epsilon_{abc} N^\dagger (\boldsymbol{\tau} \cdot \hat{\boldsymbol{\pi}} \vec{\nabla}_a + \overleftarrow{\nabla}_a \boldsymbol{\tau} \cdot \hat{\boldsymbol{\pi}}) \sigma_b N N^\dagger \sigma_c N \\ & + i \hat{D}_{1f} \epsilon_{abc} N^\dagger \boldsymbol{\tau} \cdot \hat{\boldsymbol{\pi}} \sigma_b N N^\dagger \sigma_c (\vec{\nabla}_a + \overleftarrow{\nabla}_a) N \\ & + \hat{D}_{1g} N^\dagger [\boldsymbol{\tau} \cdot \hat{\boldsymbol{\pi}} \vec{\sigma} \cdot \vec{\nabla} + \vec{\sigma} \cdot \overleftarrow{\nabla} \boldsymbol{\tau} \cdot \hat{\boldsymbol{\pi}}, \tau_i] N N^\dagger \tau_i N + \hat{D}_{1h} N^\dagger [\boldsymbol{\tau} \cdot \hat{\boldsymbol{\pi}} \vec{\sigma}, \tau_i] N \cdot N^\dagger (\vec{\nabla} + \overleftarrow{\nabla}) \tau_i N \\ & \left. + i \hat{D}_{1i} \epsilon_{abc} N^\dagger [\boldsymbol{\tau} \cdot \hat{\boldsymbol{\pi}} \vec{\nabla}_a - \overleftarrow{\nabla}_a \boldsymbol{\tau} \cdot \hat{\boldsymbol{\pi}}, \tau_i] \sigma_b N N^\dagger \sigma_c \tau_i N \right\} , \end{aligned} \quad (9)$$

where  $\hat{D}_{1a} - \hat{D}_{1i}$  are dimensionless coupling constants. These counter terms are next-to-next-to-leading order ( $N^2$ LO) terms in the chiral  $s$ -wave pion production operator.

We explicitly calculate the WRG running of the coefficients of the leading chiral counter terms ( $\hat{D}_{1a} - \hat{D}_{1i}$  in Eq. (9)) for an infinitesimal reduction of the cutoff; the LO chiral nuclear force is used together. The details of the calculation and the result are given in the Appendix. This calculation also illustrates that no CSV terms (such as Eq. (25) in Ref. [20]<sup>6</sup>) are generated in the WRG running. Here, we generalize the result and exclude a possibility that the WRG running generates a CSV term, provided that the starting operator does not include a CSV term. In Eq. (3), the second, third and fourth terms, which we will refer to as the generated terms, are to be captured by the counter terms. This part is linear in the starting operator. From Eq. (6), we see that the starting operator is proportional to the pion energy and so are the generated terms. Thus, the counter terms include the time derivative of the pion field. Meanwhile, the starting operator and the full Hamiltonian have symmetries such as hermiticity, rotational invariance and parity, and the RG running maintains these symmetries. To be consistent with the symmetries, each of the generated terms has to include a pseudoscalar factor formed by the spatial derivatives and the nucleon spin operators. In fact, the heavy-baryon  $\chi$ PT Lagrangian always includes such counter

---

<sup>6</sup> Discussion in the first paragraph of Sec. III gives a reason why the authors of Ref. [20] obtained the CSV term.

terms which are the most general terms consisting of the time derivative of the pion field and four nucleon fields. Thus no CSV terms are generated in the WRG running.

Using the result in the appendix, we can (roughly) infer the size of the running in case the cutoff is reduced by a certain finite amount. Consider the running of the counter terms driven by  $O_{\text{WT}'}$  [Eq. (6)] and the one-pion-exchange potential ( $V_{\text{OPEP}}$ ) [Eq. (A.1)]. For an infinitesimal reduction of the cutoff, the running of the counter terms is given by Eq. (A.6). Integrating over  $\Lambda$  from  $\bar{\Lambda}$  down to  $\Lambda$  ( $\bar{\Lambda} > \Lambda$ ) gives

$$\hat{D}_{1a}^{(1\text{-loop})} = \frac{4 g_A^2 M^3}{3 (4\pi f_\pi)^2 m_\pi} \left\{ \arctan\left(\frac{\bar{\Lambda}}{m_\pi}\right) - \arctan\left(\frac{\Lambda}{m_\pi}\right) \right\}. \quad (10)$$

In case  $\bar{\Lambda} > \Lambda \gg m_\pi$ , we have

$$\hat{D}_{1a}^{(1\text{-loop})} \simeq \frac{4 g_A^2 M^3 (\bar{\Lambda} - \Lambda)}{3 (4\pi f_\pi)^2 \bar{\Lambda} \Lambda}. \quad (11)$$

The relative strength among  $\hat{D}_{1a}$  and other  $\hat{D}_{1x}$  ( $x = b, \dots, i$ ) is the same as Eq. (A.6). This is the running of the counter terms generated by the one-loop formed by  $O_{\text{WT}'}$  and  $V_{\text{OPEP}}$ , in which the internal relative momentum of the two nucleons runs from  $\bar{\Lambda}$  to  $\Lambda$ . The running of the counter terms also captures contributions from the sum of the ladder diagrams in which  $O_{\text{WT}'}$  is dressed by multiple iteration of  $V_{\text{OPEP}}$ . Such a contribution roughly gives the running coupling constant as

$$\begin{aligned} \hat{D}_{1a}^{(\text{multi-loops})} &\sim \hat{D}_{1a}^{(1\text{-loop})} \left( 1 + \frac{M(\bar{\Lambda} - \Lambda)}{(4\pi f_\pi)^2} + \left( \frac{M(\bar{\Lambda} - \Lambda)}{(4\pi f_\pi)^2} \right)^2 + \dots \right) \\ &= \hat{D}_{1a}^{(1\text{-loop})} \left( \frac{1}{1 - \frac{M(\bar{\Lambda} - \Lambda)}{(4\pi f_\pi)^2}} \right), \end{aligned} \quad (12)$$

where  $\bar{\Lambda} - \Lambda < 4\pi f_\pi$  is assumed from the first to second line. Although not explicitly shown, each term on the R.H.S. of the first line, in fact, is accompanied by a dimensionless constant factor which is  $\mathcal{O}(1)$  and is different for different terms. Even though Eq. (12) is a rather crude estimation of  $\hat{D}_{1a}^{(\text{multi-loops})}$ , it still implies a condition for the WRG running of the chiral counter terms to be of natural size:  $\bar{\Lambda} - \Lambda \ll 4\pi f_\pi$ . (We supposed that the starting chiral counter terms are of natural size.) If this condition is not satisfied, the running of the counter terms may not necessarily be finite.<sup>7</sup> Furthermore, we find that  $\bar{\Lambda} - \Lambda \ll 4\pi f_\pi$  is a condition to justify the naive expectation that the WRG running has the dependence

---

<sup>7</sup> Our argument here has a similarity to that used for identifying the chiral symmetry breaking scale ( $\Lambda_\chi$ ) with  $\Lambda_\chi \sim 4\pi f_\pi$  [23]. Both of the arguments are based on the size of the RG running. However, we do not think that there is a direct connection between the two arguments. In Ref. [23], a cutoff variation of a reasonable amount leads to a renormalization of couplings, and the size of the renormalization

on the cutoff as  $\propto 1/\Lambda$ . For a perturbative calculation, this expectation is true, irrespective of the size of  $\bar{\Lambda} - \Lambda$ , as shown in Eq. (11). In a non-perturbative calculation such as  $NN$  interaction, however, the scaling of the coupling is more complicated as seen in Eq. (12). Now we estimate the size of the generated coupling constant which should be of natural size for the counting rule to work. Taking a physically reasonable range ( $\bar{\Lambda} = 800$  MeV and  $\Lambda = 500$  MeV), which is fairly consistent with the condition obtained above ( $\bar{\Lambda} - \Lambda \ll 4\pi f_\pi$ ), we obtain with Eqs. (11) and (12)

$$\hat{D}_{1a}^{(1\text{-loop})} \sim 0.9, \quad \hat{D}_{1a}^{(\text{multi-loops})} \sim 1.2, \quad (13)$$

which are the running of natural size. The above analysis is for the leading order chiral counter terms. A similar analysis can also be applied to higher order counter terms to show that the running of the couplings is of natural size. Thus this qualitative analysis supports the consistency between the RG running and the counting rule in case the cutoff is varied within the physically reasonable range.

In this paragraph, we discuss an implication from the above analysis for the nuclear force. Consider the one-pion-exchange potential ( $V_{\text{OPEP}}$ ). The WRG running of  $V_{\text{OPEP}}$  generates a series of contact interactions with even numbers of derivatives, *i.e.*,

$$V_{\text{CT}}(\mathbf{k}', \mathbf{k}) = \frac{1}{4f_\pi^2} \left( \hat{C}_0 + \frac{\hat{C}_2}{\Lambda^2}(k^2 + k'^2) + \dots \right), \quad (14)$$

where  $\hat{C}_i$  ( $i = 0, 2, \dots$ ) are dimensionless couplings. These couplings have a RG running similar to Eq. (12). Therefore, if we reduce the cutoff within the reasonable range (*e.g.*,  $\bar{\Lambda} = 800$  MeV and  $\Lambda = 500$  MeV), the resultant renormalization of the couplings is  $\mathcal{O}(1)$ , which implies consistency between the WRG running and Weinberg's counting. However, the couplings could be divergent when the cutoff is varied by  $\bar{\Lambda} - \Lambda > 4\pi f_\pi$ . In fact, divergences of the RG running of contact  $NN$  interactions for some partial waves are indeed observed in Ref. [5] (*e.g.*, see Fig. 2 of the paper) in which the cutoff is varied over a very wide range from  $2 \text{ fm}^{-1}$  to  $20 \text{ fm}^{-1}$ ; Eq. (12) is consistent with the divergent behavior. Obviously, the counting rule does not work for the divergent contact interactions. We vary the cutoff within the physically reasonable range where the counting rule is not broken by the divergence, and study the consistency between the RG running and the counting rule.

Although the above analysis based on the (semi-)analytic result suggested that the RG running of the chiral counter terms is of natural size, it was a rather crude estimation. Thus

---

( $\sim 1/(4\pi f_\pi)^2$ ) is related to the chiral symmetry breaking scale; the RG running is due to one-loop diagrams of the  $\pi\pi$  interaction (perturbative). In our case, we found the size of the cutoff variation ( $\sim 4\pi f_\pi$ ) which may take the couplings away from the natural size; the RG running here is due to the sum of the ladder diagrams of the  $NN$  interaction (non-perturbative).

it is desirable to confirm this result by a numerical calculation as follows. Starting with the chiral NLO  $\pi$ -production operator [Eq. (6)] with  $\Lambda = 800$  MeV, we reduce the cutoff down to  $\Lambda = 500$  MeV, with the use of the integral form of the WRG equation [Eq. (3)].<sup>8</sup> Then we examine whether the generated terms as a result of the WRG running are captured by the chiral counter terms in a way consistent with the counting rule. This time, we use the WRG equation [Eq. (3)] for which the partial wave decomposition has been done. Because we are interested in the  $NN \rightarrow d\pi$  reaction near threshold, we only need to consider the  ${}^3P_1 \rightarrow {}^3S_1$ - ${}^3D_1$  transition in the  $NN$  system. Since we use Eq. (3), the resultant RG effective operator does not have spin and isospin structure any more, and only the radial dependence is at hand. In fact, some of the chiral counter terms with different spin and isospin structures give the same radial dependence in our case ( ${}^3P_1 \rightarrow {}^3S_1$ - ${}^3D_1$  transition near threshold). Thus we know that the generated part includes various counter terms [Eq. (9)], but we cannot separate them in practice because they give the same radial dependence. What we can do is to use a representative of such counter terms to parameterize the generated part. Fortunately, this situation still does not ruin our goal of examining the consistency between the RG running and the counting rule. We use the following chiral counter terms as representatives for parameterizing the generated part:

$$\begin{aligned}
\mathcal{L} = & \frac{\hat{D}_{1a}}{2Mf_\pi} \frac{g_A}{Mf_\pi^2} (iN^\dagger \boldsymbol{\tau} \cdot \hat{\boldsymbol{\pi}} \vec{\sigma} \cdot \vec{\nabla} N + H.c.) N^\dagger N \\
& + \frac{\hat{D}_{3a}}{2Mf_\pi \Lambda^2} \frac{g_A}{Mf_\pi^2} (iN^\dagger \boldsymbol{\tau} \cdot \hat{\boldsymbol{\pi}} \vec{\sigma} \cdot \vec{\nabla} N + H.c.) (N^\dagger \vec{\nabla}^2 N + H.c.) \\
& + \frac{\hat{D}_{3b}}{2Mf_\pi \Lambda^2} \frac{g_A}{Mf_\pi^2} (iN^\dagger \boldsymbol{\tau} \cdot \hat{\boldsymbol{\pi}} \vec{\sigma} \cdot \vec{\nabla} N + H.c.) (\vec{\nabla} N^\dagger \cdot \vec{\nabla} N) \\
& + \frac{\hat{D}_{3c}}{2Mf_\pi \Lambda} \frac{g_A}{Mf_\pi^2} (iN^\dagger \boldsymbol{\tau} \cdot \hat{\boldsymbol{\pi}} \vec{\sigma} \cdot \vec{\nabla} N + H.c.) (N^\dagger \left( i \vec{\partial} t + \frac{\vec{\nabla}^2}{2M} \right) N + H.c.) \\
& + \frac{\hat{D}_{5a}}{2Mf_\pi \Lambda^4} \frac{g_A}{Mf_\pi^2} (iN^\dagger \boldsymbol{\tau} \cdot \hat{\boldsymbol{\pi}} \vec{\sigma} \cdot \vec{\nabla} N + H.c.) (N^\dagger (\vec{\nabla}^2)^2 N + H.c.) \\
& + \frac{\hat{D}_{5b}}{2Mf_\pi \Lambda^4} \frac{g_A}{Mf_\pi^2} (iN^\dagger \boldsymbol{\tau} \cdot \hat{\boldsymbol{\pi}} \vec{\sigma} \cdot \vec{\nabla} N + H.c.) N^\dagger (\vec{\nabla} \cdot \vec{\nabla}) (\vec{\nabla}^2 + \overleftarrow{\nabla}^2) N \\
& + \frac{\hat{D}_{5c}}{2Mf_\pi \Lambda^4} \frac{g_A}{Mf_\pi^2} (iN^\dagger \boldsymbol{\tau} \cdot \hat{\boldsymbol{\pi}} \vec{\sigma} \cdot \vec{\nabla} N + H.c.) N^\dagger (\vec{\nabla} \cdot \vec{\nabla})^2 N
\end{aligned}$$

---

<sup>8</sup> In this work, we consider a pion production near threshold where the on-shell relative momentum is about 360 MeV. Therefore, it is impossible for an operator with a cutoff less than 360 MeV to treat the pion production. Also, we should consider explicitly degrees of freedom whose details matter to a problem under consideration. Therefore, we consider 500 MeV to be an appropriate lowest value for the cutoff.

$$\begin{aligned}
& + \frac{\hat{D}_{5d}}{2Mf_\pi\Lambda^2} \frac{g_A}{Mf_\pi^2} (iN^\dagger \boldsymbol{\tau} \cdot \hat{\boldsymbol{\pi}} \vec{\sigma} \cdot \vec{\nabla} N + H.c.) (N^\dagger \left( i \vec{\partial} t + \frac{\vec{\nabla}^2}{2M} \right)^2 N + H.c.) \\
& + \frac{\hat{D}_{5e}}{2Mf_\pi\Lambda^3} \frac{g_A}{Mf_\pi^2} (iN^\dagger \boldsymbol{\tau} \cdot \hat{\boldsymbol{\pi}} \vec{\sigma} \cdot \vec{\nabla} N + H.c.) (N^\dagger (\vec{\nabla}^2 + \overleftarrow{\nabla}^2) \left( i \vec{\partial} t + \frac{\vec{\nabla}^2}{2M} \right) N + H.c.) \\
& + \frac{\hat{D}_{5f}}{2Mf_\pi\Lambda^3} \frac{g_A}{Mf_\pi^2} (iN^\dagger \boldsymbol{\tau} \cdot \hat{\boldsymbol{\pi}} \vec{\sigma} \cdot \vec{\nabla} N + H.c.) (N^\dagger (\overleftarrow{\nabla} \cdot \vec{\nabla}) \left( i \vec{\partial} t + \frac{\vec{\nabla}^2}{2M} \right) N + H.c.) , \quad (15)
\end{aligned}$$

where the  $\hat{D}_x (x = 1a, \dots, 5f)$  are dimensionless coupling constants. This is a power expansion with respect to the RG scale  $\Lambda$ , *i.e.*, in powers of  $p/\Lambda$ . We presented higher order chiral counter terms with three or five derivatives. Although there are also many spin-isospin structures possible for the counter terms with three or five derivatives, we presented only the representatives which we indeed use in parameterizing the generated part. We do not have a criterion to select the set of operators in Eq. (15). Even if we included some more operators, we would not have a better parameterization. The coefficients for those counter terms are  $\hat{D}_{3a}$ – $\hat{D}_{3c}$  and  $\hat{D}_{5a}$ – $\hat{D}_{5f}$ , where the index 3 and 5 indicate how many nucleon derivatives they have. Note that contact operators with an even number of spatial derivatives will not survive sandwiching between wave functions for the  ${}^3P_1 \rightarrow {}^3S_1$ – ${}^3D_1$  transition.

The counter terms with the LECs  $\hat{D}_{3c}$ ,  $\hat{D}_{5d}$ ,  $\hat{D}_{5e}$ , and  $\hat{D}_{5f}$  are the so-called redundant terms. The redundant terms are generated in the WRG running, as explicitly shown in the Appendix. Although those terms may be eliminated by a field redefinition, the field redefinition is accompanied by a contribution from the measure (the Jacobian factor) which is difficult to calculate [24]. Thus, we explicitly consider the redundant terms, which means that we explicitly consider the on-shell energy dependence of the low-momentum operator.

## V. NUMERICAL RESULTS

We start with the chiral NLO  $s$ -wave pion production operator for the  $NN \rightarrow d\pi$  reaction, presented in Sec III. The starting operator is defined in the model space with  $\Lambda = 800$  MeV (sharp cutoff). Using the integral form of the WRG equation in Eq. (3), we calculate the RG low-momentum operator for  $\Lambda = 500$  MeV.<sup>9</sup> Unless otherwise stated, we use the low-momentum  $NN$  potential obtained from the CD-Bonn  $NN$ -potential [10] to generate the initial proton-neutron  ${}^3P_1$  scattering and final deuteron wave functions. Some reasons for using the phenomenological nuclear force rather than a  $\chi$ PT-based nuclear force have been given in the introduction. For the purposes of this paper we can ignore any charge-dependent

---

<sup>9</sup> We may use either Eq. (2) after the partial wave decomposition, or Eq. (3) to calculate an effective RG operator; the result is the same. We use Eq. (3) for an easier calculation.

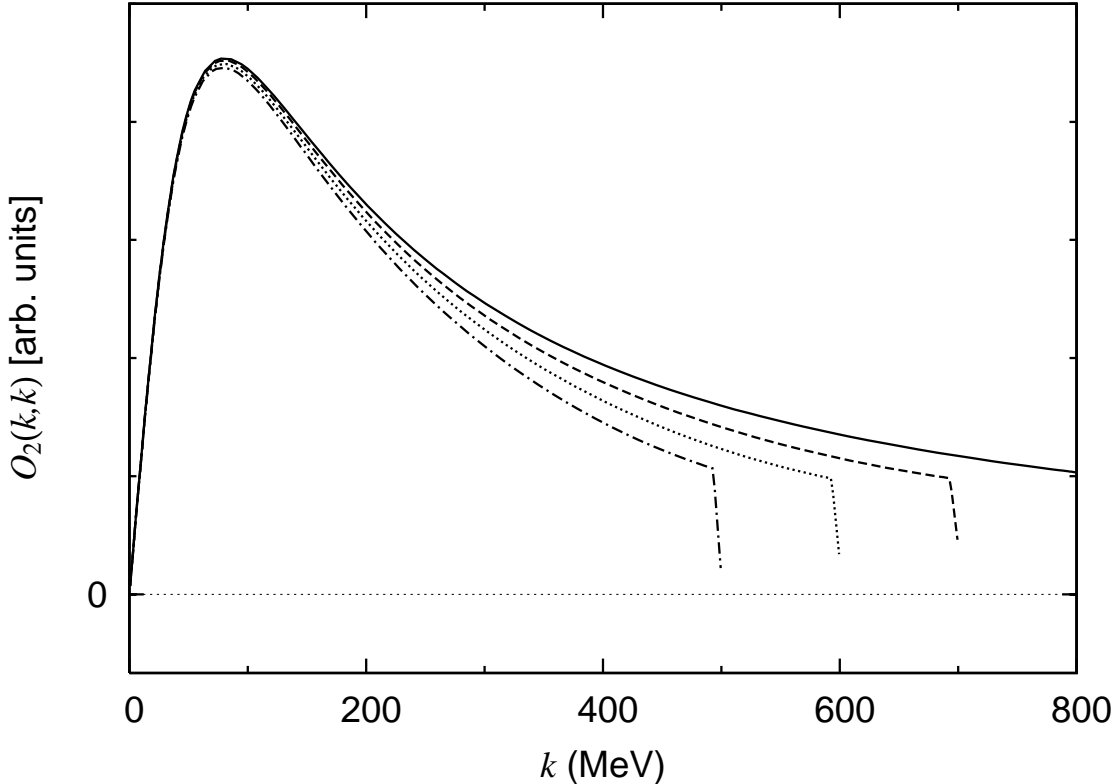


FIG. 1: Running of the pion production operator for the  ${}^3P_1 \rightarrow {}^3S_1$  transition in  $NN \rightarrow d\pi$ . The diagonal momentum space matrix elements are shown. The starting chiral NLO operator ( $\Lambda = 800$  MeV) is shown by the solid line. After the RG running, we obtain the low-momentum operator with  $\Lambda = 700$  MeV (dashed line),  $\Lambda = 600$  MeV (dotted line), and  $\Lambda = 500$  MeV (dash-dotted line);  $\eta = 0.1$ . The abrupt drop in the curves close to the cutoff is a reflection of our treatment of the one-body operator (the kink structure).

effects and assume that our calculation (of  $np \rightarrow d\pi^0$ ) applies equally well to (Coulomb-corrected)  $pp \rightarrow d\pi^+$ . Thus we will consistently write  $NN \rightarrow d\pi$ . We also employ near threshold kinematics, *i.e.*,  $\eta \sim 0.1$ , where  $\eta = q/m_\pi$  is the emitted pion momentum divided by the pion mass. The chiral counter terms that we use to simulate the generated part of the RG low-momentum operator have been presented in Eq. (15).

### A. The ${}^3P_1 \rightarrow {}^3S_1$ transition

The running of the radial part of the  ${}^3P_1 \rightarrow {}^3S_1$  transition operator (diagonal matrix elements) is shown in Fig. 1. The solid line is the starting NLO chiral operator (before RG running). After the RG running, we obtain the RG low-momentum operator shown by the

dashed line ( $\Lambda = 700$  MeV), dotted line ( $\Lambda = 600$  MeV) and dash-dotted line ( $\Lambda = 500$  MeV). Only the result for the diagonal components is given here—a similar trend is found for the off-diagonal components. As stated earlier, we expect to observe a kink structure, which is similar to the “jump-up” structure in Ref. [15], in the low-momentum operators. Here it actually appears up as an abrupt drop close to the cutoff.

Now we parameterize this low-momentum operator using the NLO operator plus the counter terms in Eq. (15). We omit the kink part when fitting the counter terms. Since the low-momentum operator has the on-shell energy dependence, we also need to include the redundant terms in our fit. The low-momentum operator is calculated for a range in  $\eta$  between 0.02 and 0.1 with steps of 0.02. We fit the LECs to these low-momentum operators using the least squares method and with both diagonal and off-diagonal matrix elements as input. The  $\eta$ -dependence is then parameterized by the redundant terms. All momenta smaller than  $\Lambda$  are used with equal weight in the fitting.<sup>10</sup> The LECs obtained in this way are presented in Table I. We notice that  $\hat{D}_{1a}$  changes significantly when adding the  $\hat{D}_{3x}$  terms. This is a consequence of introducing the redundant term  $\hat{D}_{3c}$ . A similar change is observed also in  $\hat{D}_{3a}$ ,  $\hat{D}_{3b}$ , and  $\hat{D}_{3c}$  as the  $\hat{D}_{5x}$  terms are added. The LECs in Table I are used to obtain the results in the following figures and tables.

In Fig. 2, we show the simulation of the low-momentum operator using the NLO operator plus the counter terms. The dash-dotted line is the starting NLO chiral operator and the solid line is the low-momentum operator. The dashed line contains the NLO operator plus the counter term with coefficient  $\hat{D}_{1a}$ . The dotted line contains the additional terms  $\hat{D}_{3a}$ ,  $\hat{D}_{3b}$ , and  $\hat{D}_{3c}$  of Eq. (15). The generated part (the difference between the solid and dash-dotted lines) is thus accurately captured by the higher order counter terms. In addition, the size of the dimensionless couplings is natural as can be gleaned from Table I, where we also include five derivatives counter terms.<sup>11</sup> The natural sizes of the LECs show that the chiral expansion of the contact operator indeed converges very well, confirming the visual information in Fig. 2.

Because of the large momentum mismatch between the initial and final on-shell momenta

---

<sup>10</sup> In principle the smaller momentum should have larger weight in the fitting, since in an effective theory the low-momentum behavior of the operator is more accurately described. However, as we will see shortly, we can easily achieve a good fit for the full range  $< \Lambda$ . Therefore we do not think it necessary to put heavier weight on the smaller momenta.

<sup>11</sup> The LECs  $\hat{D}_{5c}$  and  $\hat{D}_{5f}$  are relatively large, although not disturbingly so. However, because of the operator structure, the  $\hat{D}_{5c}$ -term appears with a factor 1/3 in the  ${}^3P_1 \rightarrow {}^3S_1$  transition matrix element. The  $\hat{D}_{5f}$ -term has a factor  $\Lambda/M$ , compared to the  $\hat{D}_x$ -terms ( $x = 5a, 5b, 5c$ ), which makes its contribution smaller by a factor of  $\sim 2$ . Therefore, the seemingly large LECs are ascribable to the result of the coefficients which accompany the LECs.

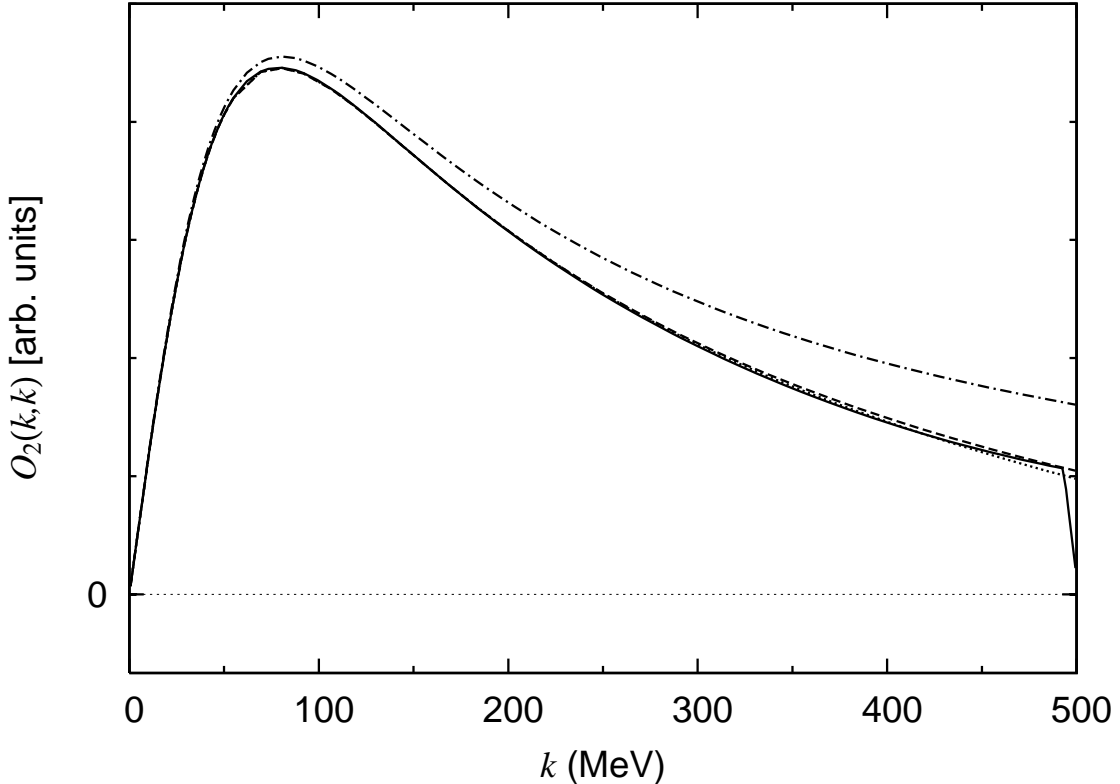


FIG. 2: Simulation of the low-momentum pion production operator ( $\Lambda = 500$  MeV,  $\eta = 0.1$ ) for the  ${}^3P_1 \rightarrow {}^3S_1$  transition in  $NN \rightarrow d\pi$ . The diagonal matrix elements are shown. The low-momentum operator (solid line) is simulated by the original NLO operator (one-body and rescattering terms, dash-dotted line) plus a contact term with one nucleon derivative (dashed line). The dotted line has additional contact terms with three derivatives.

in  $NN \rightarrow d\pi$ , the off-diagonal components are actually more important than the diagonal ones. The results for the off-diagonal matrix elements are shown in Fig. 3. The low-momentum RG operator is again well parameterized using the higher order counter terms. A similar trend is seen also for the other off-diagonal components.

### B. The ${}^3P_1 \rightarrow {}^3D_1$ transition

We also examine the running of the operator for the  ${}^3P_1 \rightarrow {}^3D_1$  transition. The result is shown in Fig. 4, where the diagonal matrix elements of the operator are given. A counter term needs to have at least three derivatives for this transition, so the counter term ( $\hat{D}_{1a}$ ) in Eq. (15) does not contribute. We simulate the low-momentum operator using the counter term ( $\hat{D}_{3b}$ )—the  $\hat{D}_{3a}$  and  $\hat{D}_{3c}$  terms cannot contribute. We choose the LECs in the same way as described in the previous subsection. This fit can be done independently of the fit of



TABLE I: The coupling constants  $\hat{D}_x$  for  $\Lambda = 500$  MeV. The first column is the transition which the counter terms induce. In the second column, “1” means that we use the counter term with one nucleon derivative in simulating the low-momentum operator. For “3” (“5”), we additionally use the counter terms with three (three and five) derivatives.

	# of $\nabla$	$\hat{D}_{1a}$	$\hat{D}_{3a}$	$\hat{D}_{3b}$	$\hat{D}_{3c}$	$\hat{D}_{5a}$
${}^3P_1 \rightarrow {}^3S_1$	1	0.77	-	-	-	-
	3	0.39	-0.64	0.70	1.31	-
	5	0.42	-0.24	1.98	0.44	0.52
${}^3P_1 \rightarrow {}^3D_1$	3	-	-	-1.37	-	-
	5	-	-	-1.21	-	-
	# of $\nabla$	$\hat{D}_{5b}$	$\hat{D}_{5c}$	$\hat{D}_{5d}$	$\hat{D}_{5e}$	$\hat{D}_{5f}$
${}^3P_1 \rightarrow {}^3S_1$	5	5.63	7.63	2.39	-2.08	-8.19
${}^3P_1 \rightarrow {}^3D_1$	5	0.93	-1.62	-	-	-1.58

the  ${}^3P_1 \rightarrow {}^3S_1$  transition operator since the other counter terms not shown in Eq. (15) now contribute in a different linear combination. Already the one-parameter-fit (dashed line) is fairly accurate. When we include the counter terms with five derivatives, we obtain an almost perfect simulation as shown by the dotted line in Fig. 4. Also these  $\hat{D}_x$  are natural (see Table I). The same level of accuracy is also observed in the simulation of the off-diagonal components.

### C. Matrix Elements

We present in Table II the matrix elements of the parameterized low-momentum operator to show the accuracy of the parametrization using the counter terms. It is clear that the counter terms accurately absorb the generated part of the low-momentum operator—already with the first counter term the expansion deviates from the low-momentum operator with only 1%. With further higher order counter terms included, the matrix elements of the low-momentum operator and its parametrization become practically indistinguishable. The convergence of the counter term expansion is thus very good.

In Table III, the values for the matrix element of each component of the operator are given to show the significance of the contribution from the generated terms. At  $\Lambda = 500$  MeV, the generated part contributes by as much as 11%. This significant contribution for the

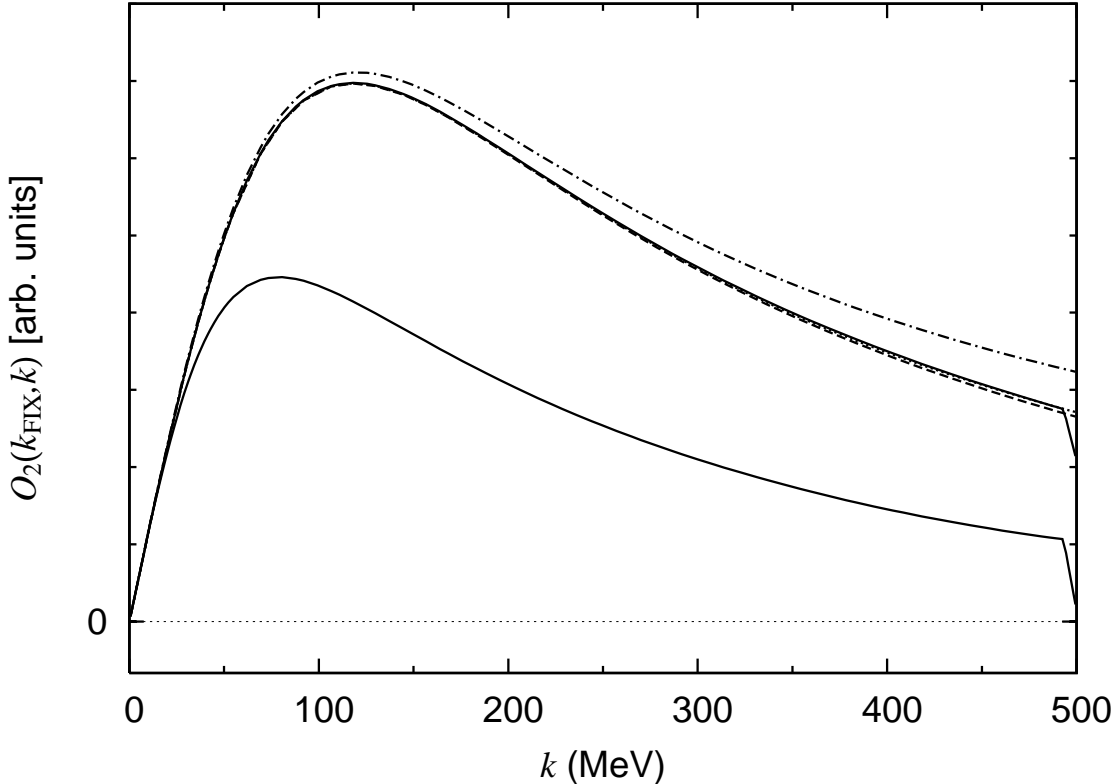


FIG. 3: Simulation of the low-momentum pion production operator ( $\Lambda = 500$  MeV,  $\eta = 0.1$ ) for the  ${}^3P_1 \rightarrow {}^3S_1$  transition in  $NN \rightarrow d\pi$ . The off-diagonal momentum space matrix elements are shown for  $k_{\text{FIX}} = 10$  MeV. The diagonal components are also shown by the lower solid line. The other features are the same as in Fig. 2.

relatively small cutoff ( $\Lambda = 500$  MeV) can be expected, because the cutoff is fairly close to the on-shell momentum of the initial  $NN$  state ( $p \sim \sqrt{Mm_\pi} \approx 360$  MeV). Thus,  $NN$  states which considerably contribute to the reaction have been integrated out and their strength shifted to contact terms.

#### D. Wave-function dependence

In this subsection we investigate the sensitivity of our result to variations in the  $NN$  potential. Using the AV18 [25] and the Nijmegen I [26] potentials, instead of the CD-Bonn potential, we again study the running of the chiral NLO operator. The result is shown in Fig. 5 together with the earlier result for the CD-Bonn potential for comparison. Obviously, the NLO operator evolves to different low-momentum operators, depending on the choice of nuclear potentials. This result is understandable since the matrix element of the chiral NLO

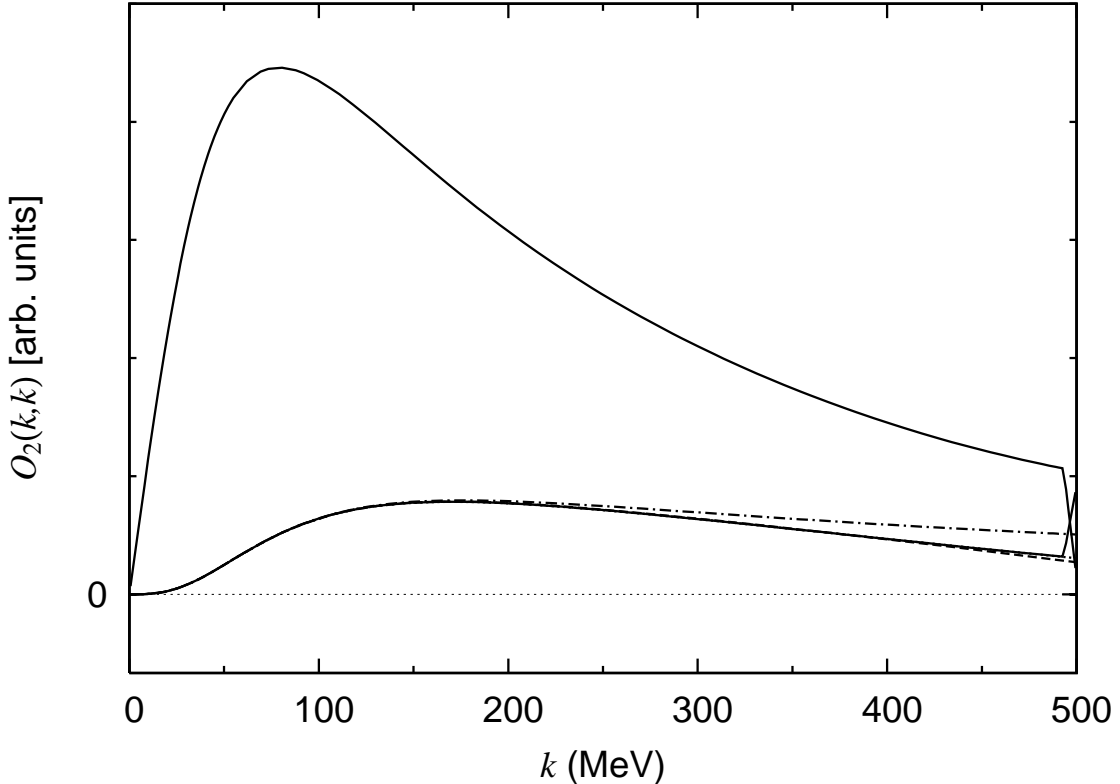


FIG. 4: Simulation of the low-momentum pion production operator ( $\Lambda = 500$  MeV,  $\eta = 0.1$ ) for the  ${}^3P_1 \rightarrow {}^3D_1$  transition in  $NN \rightarrow d\pi$ . The diagonal momentum space matrix elements are shown. The low-momentum operator (lower solid line) is simulated by the original NLO operator (one-body and rescattering terms, dash-dotted line) plus a contact term with the  $\hat{D}_{3b}$  coefficient (dashed line). The dotted line, which almost falls on the solid line, additionally includes counter terms with five derivatives. The operator for the  ${}^3P_1 \rightarrow {}^3S_1$  transition is shown for comparison (upper solid line).

operator ( $\Lambda = 800$  MeV) rather depends on the choice of the nuclear force, as demonstrated in Table IV. However, the low-momentum operators can be accurately parameterized by the chiral NLO operator plus several counter terms with the natural strength, just as we have seen in the case of the CD-Bonn potential. The accuracy of the parametrization is at a similar level regardless of potentials.

The discrepancy between the matrix elements calculated by different potentials can be regarded as a higher order effect. This is supported by the size of the differences in the cross section (Table IV), and is also confirmed by the operators—the spread in the curves of Fig. 1 stemming from RG running is similar to the spread in Fig. 5 between different wave functions.

TABLE II: Matrix elements of the pion production operator including the one-body, rescattering and several counter terms ( $\eta = 0.1$ ). In the first row, “0” includes no counter terms, i.e., it refers to the original chiral NLO operator. “1” includes the counter term with one nucleon derivative, while “3” (“5”) includes additional counter terms with three (three and five) derivatives. All matrix elements are divided by the matrix element of the RG low-momentum operator with the kink omitted, to which the counter terms are fitted.

$\Lambda$ (MeV)	0	1	3	5
700	1.02	1.01	1.00	1.00
600	1.05	1.01	1.00	1.01
500	1.11	1.01	1.00	1.00

TABLE III: Relative contributions to the matrix element from each component of the pion production operator for the original operator ( $\Lambda = 800$  MeV) and a few other cutoffs;  $\eta = 0.1$ . The symbols, “1B”, “WT’” and “Generated term” denote contributions from the one-body, modified WT term, and generated terms, respectively. The sum of all contributions is normalized to unity.

$\Lambda$ (MeV)	$\langle 1B \rangle$	$\langle WT' \rangle$	$\langle \text{Generated term} \rangle$
800	0.07	0.93	0
700	0.07	0.95	-0.02
600	0.05	1.01	-0.05
500	0.01	1.09	-0.11

In the numerical analysis presented above, the counter terms allowed by the chiral symmetry accurately simulate the generated part of the RG low-momentum operator, with the coefficients of the natural strength. We have examined the accuracy of the fitting both graphically and quantitatively (Table II). Thus, our result allows us to conclude that the RG running is consistent with the counting rule for the cutoff changed over the physically reasonable range. This result is also consistent with our (rough) semi-analytic estimation presented in Sec. IV.

## VI. SUMMARY

In nuclear  $\chi$ PT with the cutoff regularization, the cutoff has a physical meaning and its choice is not arbitrary, however, it still may be varied within a reasonable range. We examined whether the running of the counter terms, which is a result of the cutoff variation,

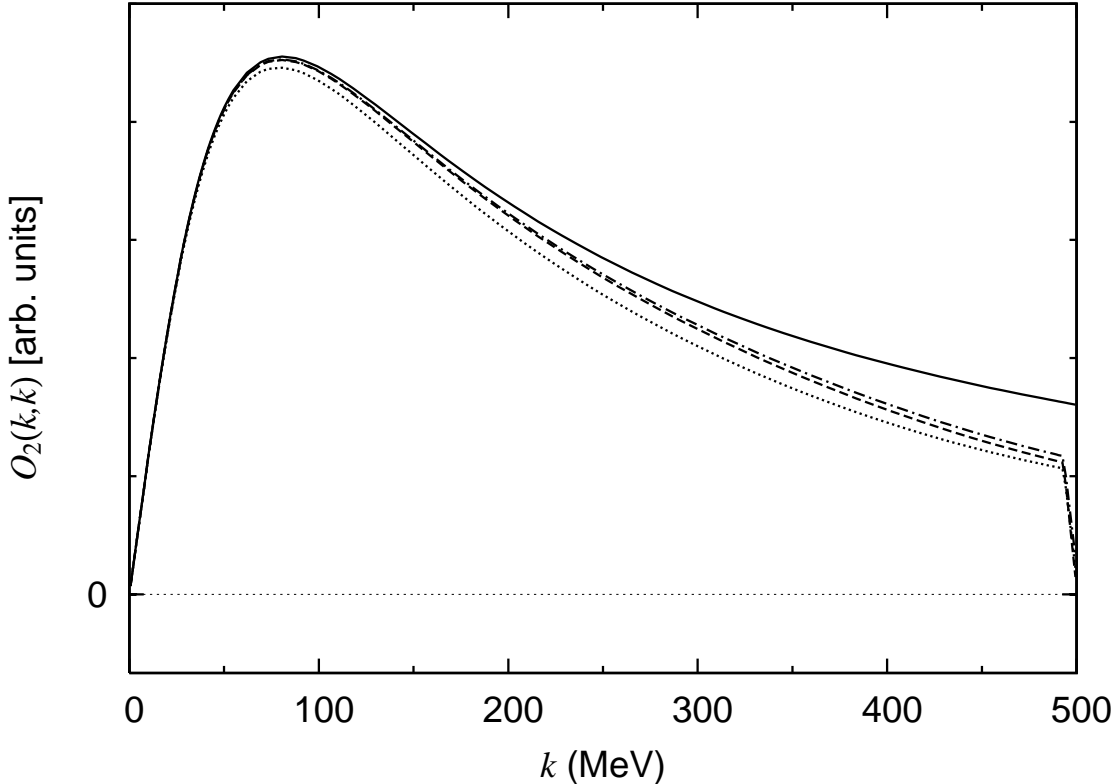


FIG. 5: Dependence of the running of the pion production operator ( ${}^3P_1 \rightarrow {}^3S_1$ ) on the choice of nuclear force for diagonal momentum space matrix elements. The original chiral NLO operator (solid line) evolves to the dashed (AV18), dash-dotted line (Nijmegen I), or the dotted (CD-Bonn) line. The cutoff value for the low-momentum operators is  $\Lambda = 500$  MeV;  $\eta = 0.1$ .

TABLE IV: The reduced  $s$ -wave cross section,  $\alpha = \sigma/\eta|_{\eta=0}$ , for various  $NN$  potentials.

	CD-Bonn	AV18	Nijmegen I
$\alpha$ ( $\mu b$ )	237	205	224

is consistent with the counting rule. This consistency is a condition for  $\chi$ PT to be useful. We proposed to use Wilsonian RG (WRG) equation for this investigation. With the use of WRG equation, it is guaranteed that no chiral-symmetry-violating (CSV) terms are generated, provided that we start with an operator consistent with the chiral symmetry. Besides, the RG running of the operator, which exactly reflects the high momentum states integrated out, is at hand, and thus we can study the convergence of the chiral expansion of the RG running.

As a demonstration, we applied the WRG equation to the  $s$ -wave  $\pi$ -production operator. We started with the chiral NLO operator [11] with the sharp cutoff,  $\Lambda = 800$  MeV. We showed that no CSV terms are generated in the WRG running by analytically calculating the WRG running of the pion production operator for the infinitesimal reduction of the cutoff; the chiral LO nuclear force is used together. In this calculation, we used differential form of the WRG equation without the partial wave decomposition. We made the rough estimate based on the result of this analytic calculation, and found a range of the cutoff variation for which the WRG running is of natural size. We also found that the WRG running may be divergent when the cutoff is changed more than 1 GeV; the WRG running does not necessarily have a simple  $\propto 1/\Lambda$  behavior when the cutoff is changed by  $\gtrsim 1$  GeV. Therefore, for the variation of the cutoff over the physically reasonable range, the RG running is consistent with the counting rule. This argument based on the analytic calculation is also applicable to the nuclear force and other transition operators. Thus we made a remark that the WRG running of the nuclear force is also consistent with Weinberg's counting rule, as long as we are concerned with a variation of the cutoff within the reasonable range.

In order to confirm the rather rough estimate given above, we numerically calculated the running of the chiral counter terms for the variation of the cutoff over the physically reasonable range. The CD-Bonn potential is used in this calculation. The couplings of the counter terms were fitted to the RG running of the operator given by the WRG equation. We found that the parametrization in terms of the counter terms is indeed accurate. Thus, the matrix elements for the low-momentum operator can be reproduced within 1% already by including the NLO operator plus just the first ( $N^2$ LO) counter term, with further improvements when higher order counter terms are included. All the couplings of the counter terms have natural strength, and thus the running can be safely considered to be of higher order than the NLO. We also used different phenomenological  $NN$  potentials, and found that the result is essentially the same as above. As mentioned in the introduction, this result implies that the phenomenological  $NN$  potentials used do not contain a significant CSV component, and thus would serve as a support of the validity of the hybrid approach. The remaining difference in the matrix element of the NLO operator among these  $NN$  potentials can most likely be captured by the  $N^2$ LO counter terms, some of which would be fitted directly to data. Thus our result indicates that, if the cutoff is varied within the physically reasonable range, the WRG running and the counting rule are consistent, at least for this reaction and to the order we are working.

## Acknowledgments

The author acknowledges Anders Gärdestig for many useful discussions. He also thanks to Koji Harada and Shung-ichi Ando for informative discussions. This work was supported by the Natural Science and Engineering Research Council of Canada and Universidade de São Paulo.

## APPENDIX: WILSONIAN RENORMALIZATION GROUP RUNNING OF CHIRAL COUNTER TERMS

Here we show analytically that the running, based on the Wilsonian renormalization group (WRG) equation, of a pion production operator is captured by the renormalization of the chiral counter terms, provided that we start with a pion production operator consistent with chiral symmetry; the operator vanishes at threshold and the chiral limit. We use the differential form of the WRG equation [Eq. (2)] to study what operators are generated as a result of the RG running. We use here the WRG equation without partial wave decomposition in order to easily identify the operator structure of the resultant operators. We examine the running of the chiral NLO  $s$ -wave  $\pi$  production operator given in Eq. (6). For the  $NN$  interaction, we use the chiral LO  $NN$  interaction, given as:

$$V_\Lambda(\mathbf{k}', \mathbf{k}; p) = -\boldsymbol{\tau}_1 \cdot \boldsymbol{\tau}_2 \frac{g_A^2}{4f_\pi^2} \frac{\boldsymbol{\sigma}_1 \cdot (\mathbf{k}'_1 - \mathbf{k}_1) \boldsymbol{\sigma}_2 \cdot (\mathbf{k}_2 - \mathbf{k}'_2)}{(\mathbf{k}'_1 - \mathbf{k}_1)^2 + m_\pi^2} + C_S(\Lambda) + C_T(\Lambda) \boldsymbol{\sigma}_1 \cdot \boldsymbol{\sigma}_2, \quad (\text{A.1})$$

with  $\mathbf{k}'_1 - \mathbf{k}_1 = \mathbf{k}_2 - \mathbf{k}'_2 = \mathbf{k}' - \mathbf{k}$ ;  $\mathbf{k}_i(\mathbf{k}'_i)$  is the momentum of the  $i$ -th nucleon before (after) the interaction. The first term is the one-pion-exchange potential ( $V_{\text{OPEP}}$ ) and the second and third terms are contact interactions with different dependences on the nuclear spin. The couplings of the contact interactions are functions of  $\Lambda$ . We start with the set of the  $NN$  potential and the  $\pi$  production operator specified above. The operators are defined in the model space with the cutoff  $\Lambda$ . We reduce  $\Lambda$  by an infinitesimal amount  $|\delta\Lambda|$ , and see the running of the  $\pi$  production operator,  $\delta O$ . In the following, we replace  $O_\Lambda$  in Eq. (2) with either  $O_{\text{WT}'}$  or  $O_{\text{1B}}$ , and  $V_\Lambda$  with either the  $V_{\text{OPEP}}$  or one of the contact interactions (we use the  $C_S$ -term only), and calculate  $\delta O$  for each combination of  $O$  and  $V$ . We will see that  $\delta O$  is captured by the renormalization of the chiral counter terms, except for the kink part from the running of  $O_{\text{1B}}$ . We show this only for the leading counter terms which have one spatial derivative. We do not explicitly calculate further higher order counter terms from  $\delta O$ . Also, our calculation of  $\delta O$  does not exhaust every possible combination of  $O$  and  $V$ . Nevertheless, our presentation is enough for our purpose of demonstrating

how the RG running is captured by the chiral counter terms. As stated in the text, no chiral-symmetry-violating terms are generated by the RG running anyway. We perform the following calculation for the threshold kinematics. Above the threshold, the starting operators in Eq. (6) have the dependence on the center-of-mass momentum even when we set the initial state in the center of mass system, and thus the resultant generated term also has the dependence on it. This dependence leads to an additional renormalization of the chiral counter terms.

1.  $O = O_{\text{WT}'}$  and  $V = V_{\text{OPEP}}$

$$\begin{aligned} \delta O_{\Lambda}^{(1)}(\mathbf{k}', \mathbf{k}; p', p) &= -|\delta\Lambda|M \left( -\frac{g_A^2}{4f_\pi^2} \right) \left( \frac{g_A m_\pi}{4f_\pi^3} \right) \int \frac{d\Omega_{\hat{\Lambda}}}{(2\pi)^3} \\ &\times \left( \frac{\boldsymbol{\sigma}_1 \cdot (\mathbf{k}'_1 - \boldsymbol{\Lambda}) \boldsymbol{\sigma}_1 \cdot (\boldsymbol{\Lambda} - \mathbf{k}_1) \boldsymbol{\sigma}_2 \cdot (\boldsymbol{\Lambda} + \mathbf{k}_2)}{[m_\pi'^2 + (\mathbf{k}'_1 - \boldsymbol{\Lambda})^2][m_\pi^2 + (\boldsymbol{\Lambda} - \mathbf{k}_1)^2](1 - p^2/\Lambda^2)} \epsilon_{abc} \tau_1^b \tau_2^c (\boldsymbol{\tau}_1 \cdot \boldsymbol{\tau}_2) \right. \\ &+ \left. \frac{\boldsymbol{\sigma}_1 \cdot (\mathbf{k}'_1 - \boldsymbol{\Lambda}) \boldsymbol{\sigma}_2 \cdot (-\mathbf{k}'_2 - \boldsymbol{\Lambda}) \boldsymbol{\sigma}_1 \cdot (\boldsymbol{\Lambda} - \mathbf{k}_1)}{[m_\pi^2 + (\mathbf{k}'_1 - \boldsymbol{\Lambda})^2][m_\pi'^2 + (\boldsymbol{\Lambda} - \mathbf{k}_1)^2](1 - p'^2/\Lambda^2)} (\boldsymbol{\tau}_1 \cdot \boldsymbol{\tau}_2) \epsilon_{abc} \tau_1^b \tau_2^c \right) + (1 \leftrightarrow 2), \quad (\text{A.2}) \end{aligned}$$

where the factor  $(-|\delta\Lambda|)$  means the infinitesimal *reduction* of the cutoff.  $\delta O_{\Lambda}^{(1)}$  is captured by a series of the counter terms. In order to see this more clearly, we expand the factors in the denominator as follows:

$$\begin{aligned} \frac{1}{m_\pi^2 + (\mathbf{k} - \boldsymbol{\Lambda})^2} &= \frac{1}{m_\pi^2 + \Lambda^2 + k^2 - 2\boldsymbol{\Lambda} \cdot \mathbf{k}} \\ &= \frac{1}{m_\pi^2 + \Lambda^2} - \frac{k^2 - 2\boldsymbol{\Lambda} \cdot \mathbf{k}}{(m_\pi^2 + \Lambda^2)^2} + \dots, \quad (\text{A.3}) \end{aligned}$$

$$\frac{1}{1 - p^2/\Lambda^2} = 1 + p^2/\Lambda^2 - \dots, \quad (\text{A.4})$$

and so on. The expansion in Eq. (A.4) generates the on-shell momentum dependent terms which are to be captured by the redundant counter terms. After the expansion of Eqs. (A.3) and (A.4), we perform the angular integral of  $\hat{\Lambda}$ , eliminating the terms with odd numbers of  $\boldsymbol{\Lambda}$ . Here, we just keep terms contributing to the renormalization of the leading counter terms shown in Eq. (9). That is, we retain the leading terms of the expansion in terms of  $1/(m_\pi^2 + \Lambda^2)$  in Eq. (A.2), and take the first term in Eq. (A.4). Note that the second term in the second line of Eq. (A.3) also gives a contribution. Thus we have,

$$\begin{aligned} \delta O_{\Lambda}^{(1)}(\mathbf{k}', \mathbf{k}; p', p) &= -\frac{|\delta\Lambda|M}{6\pi^2(m_\pi^2 + \Lambda^2)} \left( -\frac{g_A^2}{4f_\pi^2} \right) \left( \frac{g_A m_\pi}{4f_\pi^3} \right) \\ &\times \left[ \{-2\boldsymbol{\sigma}_1 \cdot (\mathbf{k}_1 - \mathbf{k}'_1) + \boldsymbol{\sigma}_1 \cdot (\mathbf{k}_2 - \mathbf{k}'_2)\} \epsilon_{abc} \tau_1^b \tau_2^c \right. \\ &+ \left. \{2\boldsymbol{\sigma}_1 \cdot (\mathbf{k}_1 + \mathbf{k}'_1) - \boldsymbol{\sigma}_2 \cdot (\mathbf{k}_1 + \mathbf{k}'_1)\} (2i)(\tau_1^a - \tau_2^a) \right] + (1 \leftrightarrow 2). \quad (\text{A.5}) \end{aligned}$$



The terms generated in this way are captured by the renormalization of the chiral counter terms in Eq. (9) as follows:

$$\delta\hat{D}_{1a} = 2\delta\hat{D}_{1b} = -2\delta\hat{D}_{1c} = -\delta\hat{D}_{1d} = 2\delta\hat{D}_{1g} = -4\delta\hat{D}_{1h} = \frac{4g_A^2 M^3 |\delta\Lambda|}{3(4\pi f_\pi)^2 (m_\pi^2 + \Lambda^2)}. \quad (\text{A.6})$$

**2.  $O = O_{\text{WT}V}$  and  $V = C_S$**

$$\begin{aligned} \delta O_\Lambda^{(2)}(\mathbf{k}', \mathbf{k}; p', p) &= -|\delta\Lambda| M C_S(\Lambda) \left( \frac{g_A m_\pi}{4f_\pi^3} \right) \int \frac{d\Omega_{\hat{\Lambda}}}{(2\pi)^3} \left( \frac{\boldsymbol{\sigma}_1 \cdot (\mathbf{k}'_1 - \boldsymbol{\Lambda})}{[m_\pi'^2 + (\mathbf{k}'_1 - \boldsymbol{\Lambda})^2](1 - p^2/\Lambda^2)} \right. \\ &\quad \left. + \frac{\boldsymbol{\sigma}_1 \cdot (\boldsymbol{\Lambda} - \mathbf{k}_1)}{[m_\pi'^2 + (\boldsymbol{\Lambda} - \mathbf{k}_1)^2](1 - p'^2/\Lambda^2)} \right) \epsilon_{abc} \tau_1^b \tau_2^c + (1 \leftrightarrow 2). \end{aligned} \quad (\text{A.7})$$

As done for  $\delta O_\Lambda^{(1)}$ , we keep the leading contributions  $[1/(m_\pi'^2 + \Lambda^2)]$  to obtain

$$\delta O_\Lambda^{(2)}(\mathbf{k}', \mathbf{k}; p', p) = \frac{|\delta\Lambda| M C_S(\Lambda)}{6\pi^2 (m_\pi'^2 + \Lambda^2)} \left( \frac{g_A m_\pi}{4f_\pi^3} \right) \boldsymbol{\sigma}_1 \cdot (\mathbf{k}_1 - \mathbf{k}'_1) \epsilon_{abc} \tau_1^b \tau_2^c + (1 \leftrightarrow 2). \quad (\text{A.8})$$

This generated term is captured by the renormalization of the chiral counter terms:

$$\delta\hat{D}_{1g} = \frac{C_S(\Lambda) M^3 |\delta\Lambda|}{24\pi^2 (m_\pi'^2 + \Lambda^2)}. \quad (\text{A.9})$$

**3.  $O = O_{1B}$  and  $V = V_{\text{OPEP}}$**

$$\begin{aligned} \delta O_\Lambda^{(3)}(\mathbf{k}', \mathbf{k}; p', p) &= -|\delta\Lambda| M \left( -\frac{g_A^2}{4f_\pi^2} \right) \left( \frac{-ig_A m_\pi (2\pi)^3}{4M f_\pi} \right) \\ &\times \int \frac{d\Omega_{\hat{\Lambda}}}{(2\pi)^3} \left( \delta^{(3)}(\mathbf{k}'_2 + \boldsymbol{\Lambda}) \frac{\boldsymbol{\sigma}_1 \cdot (\mathbf{k}'_1 + \boldsymbol{\Lambda}) \boldsymbol{\sigma}_1 \cdot (\boldsymbol{\Lambda} - \mathbf{k}_1) \boldsymbol{\sigma}_2 \cdot (\boldsymbol{\Lambda} + \mathbf{k}_2)}{[m_\pi^2 + (\boldsymbol{\Lambda} - \mathbf{k}_1)^2](1 - p^2/\Lambda^2)} \tau_1^a (\boldsymbol{\tau}_1 \cdot \boldsymbol{\tau}_2) \right. \\ &\quad \left. + \delta^{(3)}(-\boldsymbol{\Lambda} - \mathbf{k}_2) \frac{\boldsymbol{\sigma}_1 \cdot (\mathbf{k}'_1 - \boldsymbol{\Lambda}) \boldsymbol{\sigma}_2 \cdot (-\mathbf{k}'_2 - \boldsymbol{\Lambda}) \boldsymbol{\sigma}_1 \cdot (\boldsymbol{\Lambda} + \mathbf{k}_1)}{[m_\pi^2 + (\mathbf{k}'_1 - \boldsymbol{\Lambda})^2](1 - p'^2/\Lambda^2)} (\boldsymbol{\tau}_1 \cdot \boldsymbol{\tau}_2) \tau_1^a \right) + (1 \leftrightarrow 2) \end{aligned} \quad (\text{A.10})$$

We perform the angular integral ( $\hat{\Lambda}$ ) to obtain

$$\begin{aligned} \delta O_\Lambda^{(3)}(\mathbf{k}', \mathbf{k}; p', p) &= -\frac{|\delta\Lambda| M}{\Lambda^2} \left( -\frac{g_A^2}{4f_\pi^2} \right) \left( \frac{-ig_A m_\pi}{4M f_\pi} \right) \\ &\times \left( \delta(k'_2 - \Lambda) \frac{\boldsymbol{\sigma}_1 \cdot (\mathbf{k}'_1 - \mathbf{k}'_2) \boldsymbol{\sigma}_1 \cdot (-\mathbf{k}'_2 - \mathbf{k}_1) \boldsymbol{\sigma}_2 \cdot (-\mathbf{k}'_2 + \mathbf{k}_2)}{m_\pi^2 + (\mathbf{k}'_2 + \mathbf{k}_1)^2} \tau_1^a (\boldsymbol{\tau}_1 \cdot \boldsymbol{\tau}_2) \right. \\ &\quad \left. + \delta(\Lambda - k_2) \frac{\boldsymbol{\sigma}_1 \cdot (\mathbf{k}'_1 + \mathbf{k}_2) \boldsymbol{\sigma}_2 \cdot (-\mathbf{k}'_2 + \mathbf{k}_2) \boldsymbol{\sigma}_1 \cdot (-\mathbf{k}_2 + \mathbf{k}_1)}{m_\pi^2 + (\mathbf{k}'_1 + \mathbf{k}_2)^2} (\boldsymbol{\tau}_1 \cdot \boldsymbol{\tau}_2) \tau_1^a \right) + (1 \leftrightarrow 2) \end{aligned} \quad (\text{A.11})$$

We obtained the operators with the  $\delta$ -function. This term gives the kink structure found in the text, and is not captured by the chiral counter terms. We will see later that the RG running of  $\delta O_\Lambda^{(3)}$  generates the chiral counter terms.

4.  $O = O_{1B}$  and  $V = C_S$

$$\begin{aligned}
\delta O_{\Lambda}^{(4)}(\mathbf{k}', \mathbf{k}; p', p) &= -|\delta\Lambda|MC_S(\Lambda) \left( \frac{-ig_A m_{\pi}(2\pi)^3}{4Mf_{\pi}} \right) \int \frac{d\Omega_{\hat{\Lambda}}}{(2\pi)^3} \left( \delta^{(3)}(\mathbf{k}'_2 + \Lambda) \frac{\boldsymbol{\sigma}_1 \cdot (\mathbf{k}'_1 + \Lambda)}{1 - p^2/\Lambda^2} \right. \\
&\quad \left. + \delta^{(3)}(-\Lambda - \mathbf{k}_2) \frac{\boldsymbol{\sigma}_1 \cdot (\Lambda + \mathbf{k}_1)}{1 - p'^2/\Lambda^2} \right) \tau_1^a + (1 \leftrightarrow 2) \\
&= -\frac{|\delta\Lambda|MC_S(\Lambda)}{\Lambda^2} \left( \frac{-ig_A m_{\pi}}{4Mf_{\pi}} \right) (\delta(k'_2 - \Lambda) \boldsymbol{\sigma}_1 \cdot (\mathbf{k}'_1 - \mathbf{k}'_2) \\
&\quad + \delta(\Lambda - k_2) \boldsymbol{\sigma}_1 \cdot (\mathbf{k}_1 - \mathbf{k}_2)) \tau_1^a + (1 \leftrightarrow 2) . \tag{A.12}
\end{aligned}$$

5.  $O = \delta O_{\Lambda}^{(3)}$  and  $V = C_S$

In Eqs. (A.11) and (A.12), we obtained the operators with the  $\delta$ -function. The use of the WRG equation [Eq. (2)] once more gives the counter terms as follows:

$$\begin{aligned}
\delta O_{\Lambda}^{(5)}(\mathbf{k}', \mathbf{k}; p', p) &= -MC_S(\Lambda)(-) \frac{|\delta\Lambda|M}{\Lambda^2} \left( -\frac{g_A^2}{4f_{\pi}^2} \right) \left( \frac{-ig_A m_{\pi}}{4Mf_{\pi}} \right) \int \frac{d\Omega_{\hat{\Lambda}}}{(2\pi)^3} \\
&\times \left( |\delta\Lambda|\delta(k'_2 - \Lambda) \frac{\boldsymbol{\sigma}_1 \cdot (\mathbf{k}'_1 - \mathbf{k}'_2) \boldsymbol{\sigma}_1 \cdot (-\mathbf{k}'_2 - \Lambda) \boldsymbol{\sigma}_2 \cdot (-\mathbf{k}'_2 - \Lambda)}{[m_{\pi}^2 + (\mathbf{k}'_2 + \Lambda)^2](1 - p^2/\Lambda^2)} \tau_1^a (\boldsymbol{\tau}_1 \cdot \boldsymbol{\tau}_2) \right. \\
&+ \frac{\boldsymbol{\sigma}_1 \cdot (\mathbf{k}'_1 - \Lambda) \boldsymbol{\sigma}_2 \cdot (-\mathbf{k}'_2 - \Lambda) \boldsymbol{\sigma}_1 \cdot (2\Lambda)}{[m_{\pi}^2 + (\mathbf{k}'_1 - \Lambda)^2](1 - p^2/\Lambda^2)} (\boldsymbol{\tau}_1 \cdot \boldsymbol{\tau}_2) \tau_1^a \\
&+ \frac{\boldsymbol{\sigma}_1 \cdot (2\Lambda) \boldsymbol{\sigma}_1 \cdot (\Lambda - \mathbf{k}_1) \boldsymbol{\sigma}_2 \cdot (\Lambda + \mathbf{k}_2)}{[m_{\pi}^2 + (-\Lambda + \mathbf{k}_1)^2](1 - p'^2/\Lambda^2)} \tau_1^a (\boldsymbol{\tau}_1 \cdot \boldsymbol{\tau}_2) \\
&\left. + |\delta\Lambda|\delta(\Lambda - k_2) \frac{\boldsymbol{\sigma}_1 \cdot (\Lambda + \mathbf{k}_2) \boldsymbol{\sigma}_2 \cdot (\Lambda + \mathbf{k}_2) \boldsymbol{\sigma}_1 \cdot (\mathbf{k}_1 - \mathbf{k}_2)}{[m_{\pi}^2 + (\Lambda + \mathbf{k}_2)^2](1 - p'^2/\Lambda^2)} (\boldsymbol{\tau}_1 \cdot \boldsymbol{\tau}_2) \tau_1^a \right) + (1 \leftrightarrow 2) \tag{A.13}
\end{aligned}$$

We perform the angular integral and keep the leading terms [ $\propto 1/(m_{\pi}^2 + \Lambda^2)$ ] to obtain

$$\begin{aligned}
\delta O_{\Lambda}^{(5)}(\mathbf{k}', \mathbf{k}; p', p) &= \frac{|\delta\Lambda|M^2 C_S(\Lambda)}{6\pi^2(m_{\pi}^2 + \Lambda^2)} \left( -\frac{g_A^2}{4f_{\pi}^2} \right) \left( \frac{-ig_A m_{\pi}}{4Mf_{\pi}} \right) \\
&\times \left[ |\delta\Lambda|\delta(k'_2 - \Lambda) \{ \boldsymbol{\sigma}_1 \cdot (\mathbf{k}'_1 - \mathbf{k}'_2) \boldsymbol{\sigma}_1 \cdot \boldsymbol{\sigma}_2 \} \tau_1^a (\boldsymbol{\tau}_1 \cdot \boldsymbol{\tau}_2) \right. \\
&+ |\delta\Lambda|\delta(\Lambda - k_2) \{ \boldsymbol{\sigma}_1 \cdot \boldsymbol{\sigma}_2 \boldsymbol{\sigma}_1 \cdot (\mathbf{k}_1 - \mathbf{k}_2) \} (\boldsymbol{\tau}_1 \cdot \boldsymbol{\tau}_2) \tau_1^a \\
&- \{ 2\boldsymbol{\sigma}_2 \cdot (\mathbf{k}_1 - \mathbf{k}'_1) + 6\boldsymbol{\sigma}_2 \cdot (\mathbf{k}_2 - \mathbf{k}'_2) - 2i(\boldsymbol{\sigma}_1 \times \boldsymbol{\sigma}_2) \cdot (\mathbf{k}_1 + \mathbf{k}'_1) \} i(\boldsymbol{\tau}_1 \times \boldsymbol{\tau}_2)^a \\
&\left. + \{ 2\boldsymbol{\sigma}_2 \cdot (\mathbf{k}_1 + \mathbf{k}'_1) + 6\boldsymbol{\sigma}_2 \cdot (\mathbf{k}_2 + \mathbf{k}'_2) - 2i(\boldsymbol{\sigma}_1 \times \boldsymbol{\sigma}_2) \cdot (\mathbf{k}_1 - \mathbf{k}'_1) \} \tau_2^a \right] + (1 \leftrightarrow 2) \tag{A.14}
\end{aligned}$$

The terms without  $\delta$ -function contribute to the renormalization of the counter terms as follows:

$$\delta \hat{D}_{1a} = 3\delta \hat{D}_{1b} = 3\delta \hat{D}_{1f} = -2\delta \hat{D}_{1g} = 6\delta \hat{D}_{1h} = -6\delta \hat{D}_{1i} = \frac{|\delta\Lambda|M^3 C_S(\Lambda) g_A^2}{8\pi^2(m_{\pi}^2 + \Lambda^2)} . \tag{A.15}$$

- 
- [1] S. R. Beane, P. F. Bedaque, W. C. Haxton, D. R. Phillips and M. J. Savage, in *At the frontier of particle physics*, edited by M. Shifman (World Scientific, 2001), vol. 1, p. 133; nucl-th/0008064; P. Bedaque and U. van Kolck, *Annu. Rev. Nucl. Part. Sci.* **52**, 339 (2002); E. Epelbaum, *Prog. Part. Nucl. Phys.* **57**, 654 (2006).
- [2] K. Kubodera and T.-S. Park, *Annu. Rev. Nucl. Part. Sci.* **54**, 19 (2004).
- [3] M. C. Birse, J. A. McGovern, and K. G. Richardson, *Phys. Lett.* **B464**, 169 (1999).
- [4] K. Harada and H. Kubo, *Nucl. Phys.* **B758**, 304 (2006).
- [5] A. Nogga, R.G.E. Timmermans and U. van Kolck, *Phys. Rev. C* **72** 054006 (2005).
- [6] E. Epelbaum, U.-G. Meißner, nucl-th/0609037.
- [7] S. X. Nakamura, *Prog. Theor. Phys.* **114**, 77 (2005).
- [8] E. Epelbaum, Walter Glöckle, A. Kruger and U.-G. Meißner, *Nucl. Phys.* **A645**, 413 (1999).
- [9] D. R. Entem and R. Machleidt, *Phys. Rev. C* **68**, 041001(R) (2003); E. Epelbaum, W. Glöckle and U.-G. Meißner, *Nucl. Phys.* **A747**, 362 (2005).
- [10] R. Machleidt, *Phys. Rev. C* **63**, 024001 (2001).
- [11] V. Lensky, V. Baru, J. Haidenbauer, C. Hanhart, A. E. Kudryavtsev, and U.-G. Meißner, *Eur. Phys. J. A* **27**, 37 (2006).
- [12] T. D. Cohen, J. L. Friar, G. A. Miller, and U. van Kolck, *Phys. Rev. C* **53**, 2661 (1996); C. Hanhart, G. A. Miller, and U. van Kolck, *Phys. Rev. Lett.* **85**, 2905 (2000).
- [13] V. Dmitrašinović, K. Kubodera, F. Myhrer, and T. Sato, *Phys. Lett. B* **465**, 43 (1999).
- [14] S. Weinberg, *Phys. Lett.* **B251**, 288 (1990); *Nucl. Phys.* **B363**, 3 (1991).
- [15] S. X. Nakamura and S. Ando, *Phys. Rev. C* **74**, 034004 (2006).
- [16] A. N. Kvinikhidze and B. Blankleider, *Phys. Rev. C* **76**, 064003 (2007).
- [17] C. Bloch and J. Horowitz, *Nucl. Phys.* **8**, 91 (1958).
- [18] S. K. Bogner, A. Schwenk, T. T. S. Kuo, and G. E. Brown, arXiv:nucl-th/0111042.
- [19] W. C. Haxton and T. Luu, *Nucl. Phys.* **A690**, 15c (2001); arXiv:nucl-th/0101022.
- [20] A. Gårdestig, D. R. Phillips and Ch. Elster, *Phys. Rev. C* **73**, 024002 (2006).
- [21] C. Hanhart, G. A. Miller, F. Myhrer, T. Sato, and U. van Kolck, *Phys. Rev. C* **63**, 044002 (2001); A. Motzke, Ch. Elster, and C. Hanhart, *Phys. Rev. C* **66**, 054002 (2002).
- [22] S. Ando, T.-S. Park, and D.-P. Min, *Phys. Lett.* **B509**, 253 (2001).
- [23] H. Georgi, *Weak Interactions and Modern Particle Theory*, (Addison-Wesley Publishing Company, Redwood City, 1984) p. 81.
- [24] K. Harada, K. Inoue, and H. Kubo, *Phys. Lett.* **B636**, 305 (2006).
- [25] R. B. Wiringa, V. G. J. Stoks, and R. Schiavilla, *Phys. Rev. C* **51**, 38 (1995).

- [26] V. G. J. Stoks, R. A. M. Klomp, C. P. F. Terheggen and J. J. de Swart, Phys. Rev. C **49**, 2950 (1994).